Dynamic relationship between the outer radiation belt and the plasmapause during March–May 2001

J. Goldstein[1], S. G. Kanekal[2], D. N. Baker[2], B. R. Sandel[3]

Abstract.

The dynamic spatial relationship between the outer radiation belt electrons and the plasmapause during the two-month period 30 March–30 May 2001 is determined using SAMPEX daily averaged fluxes of 2–6 MeV electrons and IMAGE EUV 10-min global images of the plasmasphere. In two events, severe erosion moved the plasmapause inside $L = 2$ and 2–3 days later the outer belt was located in the normal slot region. We determine on what time scale the outer belt location responds to changes in plasmapause location and find the inner extent of the outer belt matched (to within $\Delta L \approx 0.1$) with a 3.5-day running average of the plasmapause location, implying a ≥ 3.5-day loss time scale from pitch-angle scattering by plasmaspheric hiss and EMIC waves.

1. Introduction

The radiation belts are regions of magnetically trapped high-energy ions and relativistic electrons surrounding the Earth in space [*Van Allen and Frank*, 1959]. Electrons are found in two distinct zones: an inner belt nominally centered at $L = 1.5$ and an outer belt spanning $L \approx 3$–8. The inner belt is quite stable, being composed of electrons with particle lifetimes of months to years, with fluxes varying only during the most intense geomagnetic disturbances. In contrast, the state of the outer belt is highly variable, depending on a dynamic imbalance between source (energization) and loss processes [*Baker et al.*, 1994]. Proposed energization mechanisms include shocks (during large magnetic storms), adiabatic heating of sunward-transported plasma sheet particles, and heating via wave-particle resonance with chorus and ultra-low frequency (ULF) waves (see review by *Friedel et al.* [2002], and references therein). Losses occur on both rapid and slow time scales. Outer belt electron fluxes typically drop in phase with the onset of geomagnetic storms, most likely owing to pitch-angle scattering by electromagnetic ion cyclotron (EMIC) waves or whistler chorus [*Summers and Thorne*, 2003; *Lorentzen et al.*, 2000, 2001].

Between the inner and outer belts ($L \approx 2$–3) is a slot region normally devoid of energetic electrons. This slot region

is usually attributed to pitch-angle scattering of electrons inside the plasmasphere (see *Baker et al.* [2004] and references therein). The plasmasphere is a cold (1 eV) dense (10–$10{,}000$ cm^{-3}) torus of plasma that surrounds the Earth, enveloping the inner belt and slot region. The outer boundary of the plasmasphere, the plasmapause, generally moves rapidly inward during geomagnetic disturbances (a process known as plasmaspheric erosion), and gradually outward during recovery periods as ionospheric plasma slowly leaks out along magnetic field lines. Observations throughout the plasmasphere typically reveal the presence of a broadband whistler mode emission known as plasmaspheric hiss [*Thorne et al.*, 1973; *Meredith et al.*, 2004]. It is believed that pitch-angle scattering by hiss is the primary cause of the slot [*Lyons et al.*, 1972]. Thus, the outer extent of the plasmasphere should be of fundamental importance in predicting the inner extent of the outer belt electrons. Previous comparative studies have included the plasmapause location as a statistical or modeled quantity (e.g., *O'Brien et al.* [2003]). Using observations alone, *Baker et al.* [2004] showed a close relationship between the plasmapause location and the inner extent of the outer belt during the dramatic storms of October–November 2003. To examine the generality of this result, we perform similar analysis for a longer time period, using observations during geomagnetic disturbances of March–May 2001.

2. Electron radiation belts: SAMPEX

The Solar, Anomalous, and Magnetospheric Particle Explorer (SAMPEX) [*Baker et al.*, 1994] measures energetic electrons from a low altitude (520–675 km) 82-degree inclined orbit. Figure 1a shows daily-averaged SAMPEX fluxes of energetic (2–6 MeV) electrons, plotted vs. L and day of year 2001. Data are shown from day 80 (21 March) to 160 (9 June). In this interval there were four main bursts of enhanced electron flux in the outer belt ('1' through '4' in Figure 1a). Each burst was preceded by a 1-to-2-order of magnitude flux dropout.

Figure 1b contains a plot of the hourly Dst geomagnetic activity index, a rough indicator of the equatorial magnetic perturbation associated with the stormtime (disturbance) ring current. Four main disturbances ('1' through '4') line up with the four pre-burst electron flux dropouts. There are also four secondary magnetic disturbances (dotted lines in Figure 1b) which appear to be correlated with flux modulations within each of the 4 main flux enhancements. For example, the dotted line at day 98, 1200 UT lines up with a flux decrease. As mentioned in the introduction, these storm-time flux dropouts are typical. The rapid energization responsible for the bursts of enhanced flux that followed the dropouts is a topic of ongoing interest [*Friedel et al.*, 2002], but outside the scope of this study.

Before about day 87, the 2–6 MeV slot region was between $L \approx 1.7$–2.7. After day 87, the inner extent of the outer belt

[1] Space Science and Engineering Division, Southwest Research Institute, San Antonio, TX 78228 USA

[2] Laboratory for Atmospheric and Space Physics, University of Colorado at Boulder, Boulder, CO 80309 USA

[3] Lunar and Planetary Laboratory, University of Arizona, Tucson, AZ 85721 USA

moved inward, indicating outer belt electrons beginning to occupy the slot region. If the slot region exists because of pitch-angle scattering inside the plasmasphere, partial penetration of the slot region by persistent outer belt electrons must be related to a corresponding inward motion of the plasmapause during the disturbances.

3. Plasmapause location: IMAGE EUV

The extreme ultraviolet (EUV) imager onboard the Imager for Magnetopause to Aurora Global Exploration (IMAGE) satellite routinely obtains global images of the plasmasphere, with nominal spatial (temporal) resolution of 0.1 R_E (10 min) [*Sandel et al.*, 2001], and nominal lower sensitivity threshold equivalent to 4–8 He^+ cm^{-3} [*Goldstein et al.*, 2003]. Analysis of an EUV image typically involves extraction of the equatorial plasmapause L value vs. magnetic local time (MLT), with an uncertainty (for well-defined plasmapause density gradients) of 0.25 R_E or less [*Goldstein et al.*, 2003]. Examples of extracted plasmapauses are found in Figure 2.

We chose for analysis the 2-month period 30 March–30 May (days 89–150) 2001, during which IMAGE was in a polar orbit with apogee (8.2 R_E) over the north geomagnetic pole. The orbital plane migrated from noon-midnight MLT on day 89 to just east of dawn-dusk on day 150. From this period, we analyzed 1608 EUV plasmasphere images, and extracted 93,698 plasmapause L values, mostly from the night side (where the outermost density gradient tended to be steep, especially during times of high geomagnetic activity).

Figure 2 shows IMAGE EUV plasmapause data for the events labeled '1' and '2' in Figure 1b. For each event, there is a summary plot and 3 selected snapshots of the two-dimensional (2D) equatorial plasmapause shapes. The six (total) snapshots are plotted in Figures 2b, 2c, 2d, 2f, 2g, and 2h. The day of year 2001 and UT are given to the left of each snapshot. From each of the 1608 such 2D plasmapause snapshots, the minimum and mean (simple average)

plasmapause L value was extracted. Figures 2a ('Event 1') and 2e ('Event 2') each give a summary of the event in the form of a plot of the minimum and mean plasmapause L (red and blue dots, respectively) vs. day of year ('DOY'). In each summary plot, the gray line ('1' or '2') shows the time of peak Dst disturbance from Figure 1b, and the 3 green lettered lines indicate the times of the 3 selected 2D snapshots.

These two events follow the same pattern. Each event began after a period of moderate-to-quiet geomagnetic conditions during which plasmaspheric filling produced a nightside plasmapause (1) located between $L = 3$ and $L = 5$, and (2) characterized by an indistinct (shallow) outer density gradient, as indicated by the L-scatter (vs. MLT) in the extracted points of Figures 2b and 2f. Several hours after the peak disturbance time for each event (gray line) the plasmasphere was severely eroded (see Figures 2c and 2g), with a minimum per-event plasmapause (red line) well below $L = 2$. A day or so after the peak disturbance the plasmapause had recovered its original size and shape, presumably via refilling. From examination of all the EUV data, this cycle of erosion and recovery was repeated for each disturbance time shown in Figure 1b, although Events 1 and 2 depict the most severe plasmaspheric erosions from the selected 2-month period.

Other than a very small, narrow duskside plume of sunward convecting cold plasma (e.g., $L \approx 2$–4, 1500 MLT
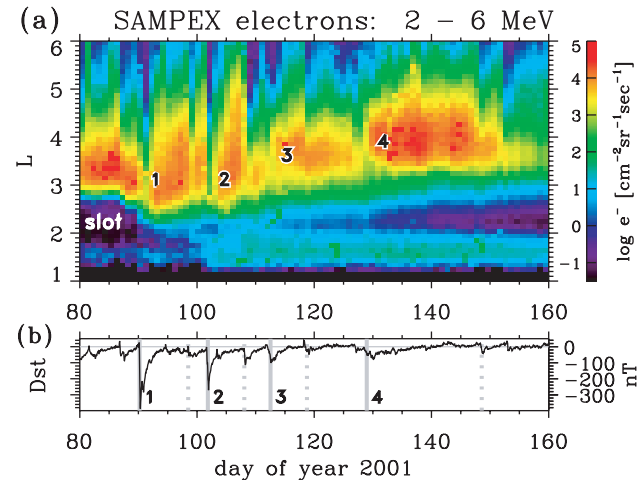
Figure 1. (a) SAMPEX high-energy (2–6 MeV) electrons, vs. L and day of year 2001. Color gives flux value according to colorbar, right of plot. Four main bursts of enhanced outer belt flux are labeled ('1' through '4'). (b) Dst index, showing 4 main disturbances ('1'–'4', gray solid lines) and 4 secondary disturbances (dotted lines).
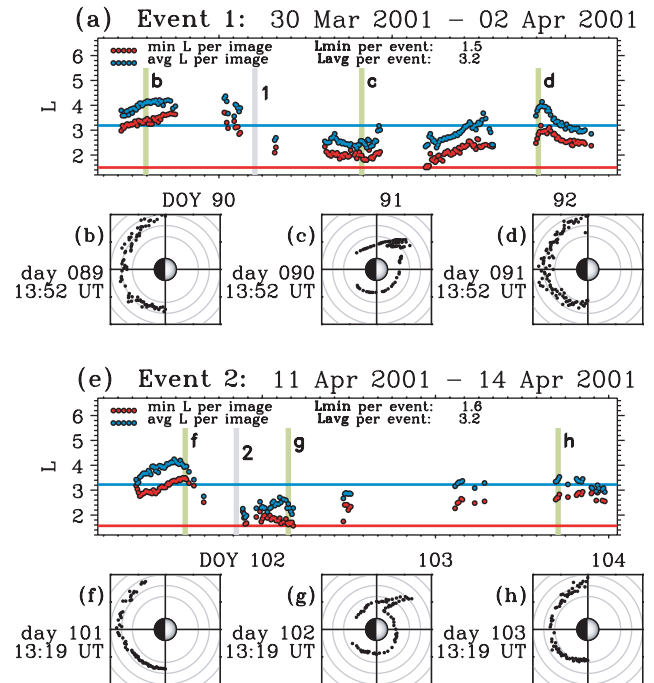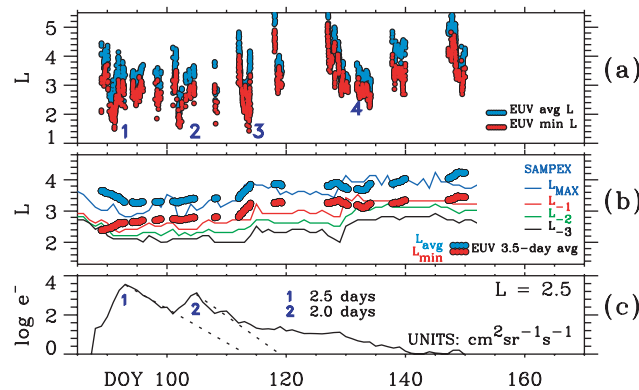

Figure 2. IMAGE EUV plasmapause data for two events from Figure 1. (a and e) Event summary plot showing minimum and mean plasmapause L (red and blue dots, respectively), per EUV image, vs. day of year. Peak Dst disturbance per event given by numbered gray line. In each summary plot, green lines indicate selected times for 3 single-image plots. Red (blue) horizontal lines: minimum (avarage) plasmapause per event. (b, c, d and f, g, h) Plasmapause L from selected single images, plotted in SM-coordinate magnetic equatorial plane. Sun to the right, Earth in center, gray circles at $L = 3, 4, 5, 6$. Day of year and UT indicated to the left of each plot.

in Figure 2g), following the extreme erosions the plasmapause was relatively round (symmetric in MLT); the minimum plasmapause was approximately the average plasmapause. In contrast, during the actual erosions (which preceded the post-erosion snapshots of Figures 2c and 2g, but were not witnessed by EUV) the plasmapause was most probably quite asymmetric in MLT. This statement is based on extensive evidence (from both models and observations) that during the actual erosion the dayside plasmasphere is pulled sunward to form a broad dayside drainage plume [*Grebowsky*, 1970; *Goldstein and Sandel*, 2005].

4. Plasmapause-outer belt relationship

Figure 3a contains minimum and average (red and blue, respectively) per-image plasmapause L_p values extracted from 1608 EUV images during 30 March–30 May 2001, in the same format as Figures 2a and 2e. The signature of plasmaspheric erosion (and subsequent recovery) is a steep drop in the minimum (or average) plasmapause L, followed by a steep rise. For example, four plasmaspheric erosions happened in phase with the four main disturbance events (labeled '1' through '4') during 30 March–30 May. Erosions (some extremely mild) also occurred during the four secondary disturbances (see dotted lines in Figure 1b).

Figure 3b compares data from SAMPEX (four solid curves) and EUV (dots) versus DOY 2001. We quantify the inner extent L_{rb} of the outer belt with L values of fractions of the peak flux. The blue line L_{MAX} is the location of the peak SAMPEX flux (f_{MAX}), and the red, green, and black lines L_{-N} show where the flux is $10^{-N} f_{MAX}$. If the slot region truly results from pitch-angle scattering by plasmaspheric hiss, then there should be a general correspondence between the inner extent of the outer belt and the plasmapause location. This correspondence should occur on a time scale set by the hiss-related loss rate. Accordingly, the red and blue dots in Figure 3b are (respectively) a 3.5-day running (boxcar) average of the minimum (L_{min}) and average (L_{avg}) per-image plasmapause L_p. By visual inspection,

good agreement is found between L_{MAX} and L_{avg} (blue line and dots), and between L_{-1} and L_{min} (red line and dots). If pitch-angle scattering is setting the inner extent of the outer belt, an important factor is the fraction of a drift orbit during which electrons at a given L-value encounter waves. Thus, the outer belt flux drops rapidly (by a factor of 10 at L_{min} and by a factor of 1000 at $L_{-3} = L_{min} - 0.7$; see caption, Figure 3b) with decreasing L inside the average plasmapause.

To further quantify this agreement, Figure 4a presents L_{MAX} vs L_{avg} (blue dots) and L_{-1} vs L_{min} (red dots), using the data from Figure 3b. The gray diagonal indicates perfect agreement. The standard deviation (ΔL) of the difference $|L_{rb} - L_p|$ (using either red or blue dots) is $\approx 0.1L$, as shown by the solid green diagonals. The average difference is $\approx 0.3L$ (dotted green diagonals). In other words, the disagreement between the outer belt and the plasmapause is comparable to the nominal EUV pixel size.

The choice of 3.5 days for the width of the EUV boxcar window was made as follows. Values of the standard deviation ΔL were computed for 50 boxcar widths between 1 and 10 days; these are plotted in Figure 4b. For short time scales (1–3 days), the ΔL curve decreases from 0.3 to 0.1, but at 3.5 days the curve levels off to a nearly constant value ~ 0.12. From this plot, the average time scale necessary for the plasmasphere to contribute to the outer belt loss rate was greater than 3.5 days for the 2-month period studied. Following *Baker et al.* [2004], the loss time scale in the slot can also be estimated directly from SAMPEX data for Events 1 and 2. Figure 3c shows $\log_{10}$ electron flux at $L = 2.5$; the dotted lines are exponential fits giving loss time scales of 2.5 days (Event 1) and 2 days (Event 2), comparable to the 4.5 day time scale obtained by *Baker et al.* [2004]. Our event-specific loss times (2–2.5 days) are slightly shorter than the average loss rate inferred for the entire 2-month period, which might mean that losses are more severe during the first two events than the rest of the 2-month period, or might reflect uncertainty in the loss time estimates.

Hiss-induced pitch-angle scattering may not have been the only plasmaspheric loss term during March–May 2001.
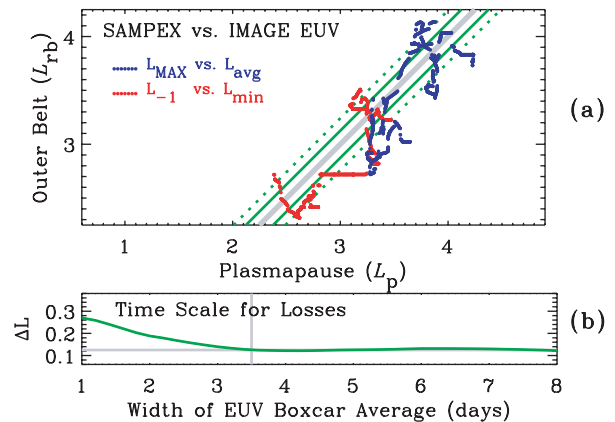

Figure 3. (a) EUV plasmapause L_p for 1608 images. Red (blue): minimum (mean) value per image. Because of the large number (1608) of data points, dots appear smeared together into line segments. (b) Red (L_{min}) and blue (L_{avg}) dots respectively give 3.5-day running (boxcar) average of minimum and mean per-image plasmapause L_p. Blue line (L_{MAX}): L of peak SAMPEX flux. Lines L_{-N} are where SAMPEX log flux drops by $-N$. On average in this plot, $L_{-3} = L_{min} - 0.7$ (c) SAMPEX log flux in slot ($L = 2.5$). Dotted lines are exponential fits indicating loss time scales for events 1 and 2.

Figure 4. (a) Empirical relationship between outer radiation belt (L_{rb}) and plasmapause (L_p) using data from Figure 3b. Blue dots: L_{MAX} vs. L_{avg}. Red dots: L_{-1} vs. L_{min}. Gray diagonal: perfect agreement. Solid green: standard deviation ΔL of $|L_{rb} - L_p|$. Dotted green: average of $|L_{rb} - L_p|$. (b) Empirical determination of electron loss time scale: standard deviation ΔL vs. width of EUV boxcar average (in days). Curve levels off to $\sim 0.12\, L$ for width >3.5 days.

A theoretical calculation by *Lyons et al.* [1972] estimated a 10 day lifetime for 2 MeV slot electrons subject to plasmaspheric whistler mode scattering alone. Plasmaspheric hiss wave amplitudes are activity dependent, reaching 30–100 pT for large (AE> 100) substorms [*Meredith et al.*, 2004]; for this hiss amplitude range *Albert* [2003] calculated electron lifetimes of 3.5–30 days. However, if EMIC wave scattering is included, the lifetimes are reduced to 0.8–4.3 days [*Albert*, 2003]. Growth of EMIC waves is favored where ring current ions overlap the plasmapause; thus, the plasmaspheric influence on the outer belt electrons may generally be a combination of both hiss (inside the plasmasphere) and EMIC wave scattering (near the plasmapause). Thus, based on available information, the 2–3.5 day loss times found for our 2-month study would require either very high amplitude hiss (not impossible for the large storms), or an EMIC wave contribution to the loss rate.

The agreement shown in Figure 4 implies that a severe plasmaspheric erosion (such that the plasmapause lies inside the nominal slot region) should provide the opportunity for electrons to occupy the slot region that normally would be devoid of electrons. Given sufficient means of energization, severe erosions will be followed by penetration of the portion of the slot region unoccupied by plasmaspheric plasma.

5.   Conclusion

Using data from SAMPEX and IMAGE EUV obtained during the 2-month period 30 March–30 May 2001, we found a close correlation between the locations of the inner extent of the outer electron radiation belt and the 3.5-day-averaged plasmapause, with a standard deviation of 0.10 L. Energization processes apparently become ineffective in the presence of hiss inside the plasmasphere and EMIC waves at the plasmapause. Plasmasphere erosion provides the opportunity (but not the certainty) for energized electrons to persist as trapped radiation belt particles; remove the plasmasphere, and the wave-related loss is removed. Thus we conclude that extreme plasmaspheric erosion (plasmapause moved inside $L \approx 2$) is a necessary, but not sufficient, condition for partial penetration of the slot region by the outer belt electrons. The average time scale for wave-related losses to control the size of the slot region is at least 3.5 days.

References

Albert, J. M. (2003), Evaluation of quasi-linear diffusion coefficients for emic waves in a multispecies plasma, *J. Geophys. Res.*, *108*(A6), 1249, doi:10.1029/2002JA009792.

Baker, D. N., J. B. Blake, L. B. Callis, J. R. Cummings, D. Hovestadt, S. Kanekal, B. Klecker, R. A. Mewaldt, and R. D. Zwicki (1994), Relativistic electron acceleration and decay time scales in the inner and outer radiation belts: SAMPEX, *Geophys. Res. Lett.*, *21*, 409.

Baker, D. N., S. G. Kanekal, X. Li, S. P. Monk, J. Goldstein, and J. L. Burch (2004), An extreme distortion of the Van Allen belt arising from the 'Halloween' solar storm in 2003, *Nature*, *432*, 878, doi:10.1038/nature03116.

Friedel, R. H. W., G. D. Reeves, and T. Obara (2002), Relativistic electron dynamics in the inner magnetosphere–A review, *J. Atmos. Solar-Terr. Phys.*, *64*, 265.

Goldstein, J., and B. R. Sandel (2005), The global pattern of evolution of plasmaspheric drainage plumes, in *Global Physics of the Coupled Inner Magnetosphere*, edited by M. Schulz, H. Spence, and J. L. Burch, American Geophysical Union, Washington, D. C., in press, PDF at http://enarc.space.swri.edu/PAPERS/PUBs/pa.pdf.

Goldstein, J., M. Spasojević, P. H. Reiff, B. R. Sandel, W. T. Forrester, D. L. Gallagher, and B. W. Reinisch (2003), Identifying the plasmapause in IMAGE EUV data using IMAGE RPI in situ steep density gradients, *J. Geophys. Res.*, *108*(A4), 1147, doi:10.1029/2002JA009475.

Grebowsky, J. M. (1970), Model study of plasmapause motion, *J. Geophys. Res.*, *75*, 4329.

Lorentzen, K. R., M. P. McCarthy, G. K. Parks, J. E. Foat, R. M. Millan, D. M. Smith, R. P. Lin, and J. P. Treilhou (2000), Precipitation of relativistic electrons by interaction with electromagnetic ion cyclotron waves, *J. Geophys. Res.*, *105*(A3), 5381.

Lorentzen, K. R., J. B. Blake, U. S. Inan, and J. Bortnik (2001), Observations of relativistic electron microbursts in association with VLF chorus, *J. Geophys. Res.*, *106*(A4), 6017.

Lyons, L. R., R. M. Thorne, and C. F. Kennel (1972), Pitch-angle diffusion of radiation belt electrons within the plasmasphere, *J. Geophys. Res.*, *77*, 3455.

Meredith, N. P., R. B. Horne, R. M. Thorne, D. Summers, and R. R. Anderson (2004), Substorm dependence of plasmaspheric hiss, *J. Geophys. Res.*, *109*, A06209, doi: 10.1029/2004JA010387.

O'Brien, T. P., K. R. Lorentzen, I. R. Mann, N. P. Meredith, J. B. Blake, J. F. Fennell, M. D. Looper, D. K. Milling, and R. R. Anderson (2003), Energization of relativistic electrons in the presence of ULF power and MeV microbursts: Evidence for dual ULF and VLF acceleration, *J. Geophys. Res.*, *108*(A8), 1329, doi:doi:10.1029/2003JA009784.

Sandel, B. R., R. A. King, W. T. Forrester, D. L. Gallagher, A. L. Broadfoot, and C. C. Curtis (2001), Initial results from the IMAGE extreme ultraviolet imager, *Geophys. Res. Lett.*, *28*, 1439.

Summers, D., and R. M. Thorne (2003), Relativistic electron pitch-angle scattering by electromagnetic ion cyclotron waves during geomagnetic storms, *J. Geophys. Res.*, *108*(A4), 1143, doi:10.1029/2002JA009489.

Thorne, R. M., E. J. Smith, R. K. Burton, and R. E. Holzer (1973), Plasmaspheric hiss, *J. Geophys. Res.*, *78*, 1581.

Van Allen, J. A., and L. A. Frank (1959), Radiation around the Earth to a radial distance of 107,400 km, *Nature*, *183*, 430.

J. Goldstein, Southwest Research Institute, 6220 Culebra Rd, San Antonio, TX 78228 USA (jgoldstein@swri.edu)

S. G. Kanekal, D. N. Baker, Lab for Atmospheric and Space Physics, U Colorado, 1234 Innovation Dr, Boulder, CO 80309 USA

B. R. Sandel, Lunar and Planetary Lab, U Arizona, 1541 E University Blvd, Tucson, AZ 85721 USA